Chemical ligation and isotope labeling to locate dynamic effects during catalysis by dihydrofolate reductase

Louis Y. P. Luk,[1] J. Javier Ruiz-Pernía,[2] Aduragbemi S. Adesina,[1] E. Joel Loveridge,[1] Iñaki Tuñón,[3,*] Vicent Moliner,[2,*] Rudolf K. Allemann[1,*]

[1] School of Chemistry, Cardiff University, Park Place, Cardiff, CF10 3AT, UK

[2] Departament de Química Física i Analítica, Universitat Jaume I, 12071 Castelló, Spain

[3] Departament de Química Física, Universitat de València, 46100 Burjassot, Spain

ABSTRACT: Experimental and computational approaches have long been employed to define the role of protein motions in enzyme catalysis, but a refined experimental method for locating the origin of dynamic effects has not previously been developed. Here a general synthetic approach is described to alter motions in specific regions of an enzyme and to analyze the effects of such localized motional changes by measuring 'segment kinetic isotope effects'. Two isotopic hybrids of dihydrofolate reductase from *Escherichia coli* (EcDHFR) were prepared by chemical ligation; one with the mobile N-terminal segment (amino acids 1-28) containing heavy isotopes (^{2}H, ^{13}C, ^{15}N) and the remainder of the protein (amino acids 29-159) with natural isotopic abundance, and the complementary hybrid with the C-terminal segment isotopically labeled. Investigation of the catalytic properties of these hybrids indicated that isotopic substitution of the N-terminal segment affects a physical step of catalysis, whereas the hydride transfer itself is affected by dynamic effects originating from residues 29-159. To verify the effectiveness of this method and to decipher its mechanistic basis, the experimental results were complemented with QM/MM computational studies, rendering a good agreement with experiments and supporting the idea of small dynamic effects on catalysis originated on the C-terminal segment. ~~which indicated that segment isotope labeling affects the recrossing trajectories on the reaction barrier~~. By isolating the effect of the motions of individual regions of the enzyme on the observed rate constants, segment kinetic isotope effects provide insight difficult to obtain with other experimental methods. Measurements of segment kinetic isotope effects will help to define the dynamic networks of intramolecular interactions central to enzyme catalysis.

INTRODUCTION

The dynamic nature of enzymes has been implicated in explaining their enormous catalytic power. Conformational changes and other motions are often critical for ligand binding and release,[1] and in several enzymes they have been shown to be important for progression through the catalytic cycle.[2-4] Inhibitors of enzyme motions might be designed that act as potent therapeutics.[5] Although it has been suggested that protein motions also play a direct role in the chemical step of the catalytic cycle,[6-10] some atomistic simulations[11-13] and experimental investigations[14-17] have suggested that models that require a non-statistical contribution from protein motions for catalysis may not be fully compatible with the available data. Indeed, simple modification of Transition State Theory (TST) is sufficient to explain the dynamic effects on the chemical step.[18-23] Recently, a combined experimental and computational analysis of protein isotope substitution, where most of the non-exchangeable isotopes in an enzyme are replaced with their heavy counterparts (^{15}N, ^{13}C and ^{2}H),[21-30] has shown that dynamic effects of the protein environment can have a measurable effect on the chemical reaction. Isotopic substitution slows protein motions from femtosecond vibrations to millisecond conformational changes without perturbing the electrostatic properties of enzymes.[24,25] Dynamic effects therefore give a measurable reactivity difference between the isotopically substituted enzyme and the 'light' enzyme with natural abundance isotope distribution.[21,22,24-30] In many cases heavy isotope substitution decreased the rate of the chemical transformation and thereby provided evidence for dynamic coupling to the reaction.[21,22,24-29]

Dihydrofolate reductase (DHFR) is a validated target for antimicrobial and anticancer drugs; the enzyme from *Escherichia coli* (EcDHFR) has been used frequently in investigations of the role of enzyme dynamics in catalysis.[19,21,22,29,31-44] EcDHFR catalyzes the formation of the cofactor tetrahydrofolate (H_4F) by transferring the pro-*R* hydride from C4 of NADPH and a solvent proton to the C-6 and N-5 positions of dihydrofolate (H_2F), respectively. The structural and catalytic properties of EcDHFR have been well characterized.[3,45,46] The M20 loop (residues 9-24) forms part of the active site and its different conformations are key to progression through the catalytic cycle (Figure 1).[3,46] Upon binding of substrate and cofactor, the M20 loop closes over the active site by forming hydrogen bonds with the FG loop (residues 116-132)[46] to create an optimal electrostatic environment for hydride transfer.[17,46] Once the products have formed, the M20 loop releases the nicotinamide ring of the oxidized cofactor and occludes part of the active site by forming an alternative hydrogen bonding pattern with the GH loop (residues 142-149),[46] which triggers the exchange of $NADP^+$ and NADPH. Finally, the M20 loop

resumes the closed conformation when the product H_4F is released.[46] However, despite its importance in EcDHFR catalysis, it has been shown that mammalian DHFRs and some other bacterial DHFRs do not form occluded conformations.[47,48]

Certain residues in the mobile loops and secondary structure elements of EcDHFR have previously been suggested to dynamically couple to the reaction coordinate.[33-35] Site-directed mutations of these residues reduced the hydride transfer rate constant significantly[33-35] and their thermal motions were shown to correlate with one another.[39,49] Experimental and theoretical investigations based on protein isotope substitution of EcDHFR indicated the nature of the dynamic coupling.[21,22] The chemical step is slower in the 'heavy' enzyme because protein motions that couple to the reaction coordinate are slower than in the 'light' enzyme. These motions do however not directly promote the reaction or enhance tunneling; instead they affect the frequency of barrier recrossing, an effect that can be described in the context of TST by including a transmission coefficient that accounts for dynamic recrossing.[21-23] Another recent report concluded that the distance between the hydride donor and acceptor remains unchanged upon protein isotope substitution in EcDHFR.[29] Computational and experimental investigations of the catalytically compromised EcDHFR-N23PP/S148A, in which motions on the timescale typical for conformational changes are lost, revealed enhanced dynamic coupling of enzyme motions on the fs-ps timescale to the reaction coordinate.[22] Such an increase in fast motions is detrimental to catalysis since it increases the number of barrier recrossing events, which in turn reduces the frequency of successful transfers from reactants to products. In all these studies the effects on the reaction of motions of the enzyme as a whole were analyzed. Here a novel experimental approach is described that allows the identification of specific enzyme regions, the motions of which affect the reaction on the timescales of both conformational changes and barrier crossings.

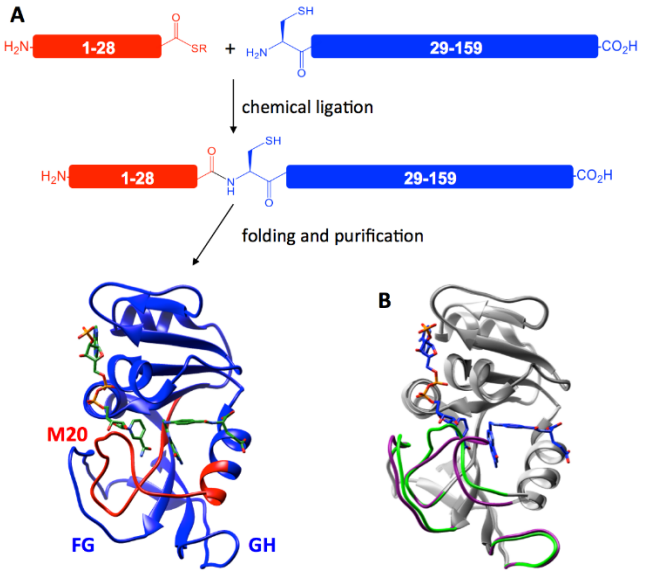

Figure 1. A) Synthesis of EcDHFR by chemical ligation (for experimental details see supporting information). The N-terminal thioester peptide (red) and C-terminal cysteine peptide (blue) are composed of residues 1-28 and residues 29-159. The M20, FG and GH loops are indicated. B) Cartoon representations of the X-ray crystal structures of EcDHFR in the closed (PDB 1RX2) and occluded (PDB 1RX4) conformations.[46] The M20, FG and GH loops are highlighted in green (closed) and purple (occluded). The ligands $NADP^+$ and folate in the closed complex are shown as sticks.

Native chemical ligation allows the construction of functional proteins *via trans*-thioesterification reactions between unprotected peptides (Figure 1).[50] It has been used to analyze the biophysical properties of proteins such as HIV protease[51] and a potassium ion channel.[52] We report here the first use of chemical ligation techniques to localize dynamic effects in hydrogen transfer reactions; to this end, EcDHFRs isotopically labeled in the N-terminal (residues 1-28; NT-EcDHFR) and C-terminal (residues 29-159; CT-EcDHFR) segments were constructed. NT-EcDHFR carries heavy isotopes (^{15}N, ^{13}C and non-exchangeable ^{2}H) in the βA strand and the active site M20 loop, whereas CT-EcDHFR possesses heavy isotopes only in the C-terminal portions of the enzyme including the FG and GH loops. Kinetic investigation of 'heavy' NT-EcDHFR and CT-EcDHFR located the regions of the enzyme responsible for dynamic coupling on the μs-ms and fs-ps timescales, while QM/MM simulations offered an explanation of the cause of dynamic coupling observed in these protein isotope labeling studies.[21-23]

RESULTS AND DISCUSSION

EcDHFR was prepared using expressed protein ligation with the reactant peptides generated by recombinant methods (Figure 1 and Figures in SI). Ala29 was changed to cysteine to serve as the nucleophile in the reaction. To verify that the Ala29 to Cys mutation did not affect the structural properties of the enzyme, wild type EcDHFR and its A29C variant were prepared and analyzed by ^{1}H-^{15}N HSQC NMR-spectroscopy (Figure S1). Only small, local differences for residues 28, 29 and 33 were observed between the spectra of the corresponding ternary $NADP^+$/folate complexes, chemical ligation was used to synthesize EcDHFR-A29C based isotopic hybrids. An N-terminal thioester peptide comprising residues 1-28 was generated in an intein-mediated approach, while the C-terminal cysteine peptide (residues 29-159) was produced using methods from a published semisynthesis of EcDHFR.[53] Ligation of the purified peptides and subsequent refolding yielded 'light' (isotopes of natural abundance) ligated EcDHFR. 'Heavy' peptides were prepared in minimal medium containing $^{2}H_2O$, ^{13}C-glucose and $^{15}NH_4Cl$. Ligation of the 'heavy' N-terminal peptide with the natural abundance C-terminal peptide yielded NT-EcDHFR, while CT-EcDHFR was obtained through chemical ligation of the natural abundance N-terminal peptide with the isotopically substituted C-terminal peptide. Mass spectrometry showed that the purified EcDHFRs were of the expected masses (Figures S2-S4). After purification in buffers made of $^{1}H_2O$, NT-EcDHFR and CT-EcDHFR showed molecular mass increases of 1.8% and 8.9%, respectively, indicating that >99.8% of the ^{14}N, ^{12}C and non-exchangeable ^{1}H atoms had been replaced by their heavier isotopes in both proteins.

The circular dichroism spectra of ligated EcDHFR, NT-EcDHFR and CT-EcDHFR revealed only minor differences to the spectrum of the wild type enzyme, suggesting that the secondary structural organization of EcDHFR is not sensitive

to the modifications made for expressed protein ligation or to isotope substitution (Figure S5), an observation that is in agreement with previous CD analyses of completely isotopically substituted EcDHFR.[21,29] However, thermal unfolding and binding kinetic investigations had shown that heavy isotope substitution can alter the ground state conformational ensemble and ligand interactions of EcDHFR.[29] Michaelis constants (K_M) of ligated EcDHFR for NADPH and H_2F were 7.6 ± 2.1 and 0.51 ± 0.06 μM (Table S1) at pH 7, similar to those of the wild type enzyme (4.8 ± 1.0 and 0.7 ± 0.2 μM, respectively).[45] The K_M values for the isotopic hybrids were similar to those of wild type EcDHFR (Table S1) with the exception of the K_M for NADPH at pH 7.0, which was reduced approximately 3-fold for NT-EcDHFR, suggesting a small segment isotope effect on cofactor binding.

The effect of segment isotopic substitution on catalytic turnover was investigated by determining steady-state rate constants (k_{cat}) at pH 7.0, where product release from the EcDHFR:NADPH:H_4F complex is mostly rate-limiting[45] (Figure 2, Figure S6 and Table S2). At 20 ºC, k_{cat} for unlabeled, ligated EcDHFR was 9.1 ± 0.3 s^{-1}, in good agreement with that measured for the wild type enzyme (8.5 ± 1.2 s^{-1}).[45] The turnover rate constant for NT-EcDHFR (k_{cat}^{NT}) was similar to that of unlabeled ligated EcDHFR (k_{cat}^{LE}) at low temperatures, but began to differ with increasing temperature. At 40 ºC, the N-terminal kinetic isotope effect ($KIE_{cat}^{NT} = k_{cat}^{LE}/k_{cat}^{NT}$) was 1.16 ± 0.05. The magnitude and temperature dependence of KIE_{cat}^{NT} were similar to those of the enzyme kinetic isotope effect ($KIE_{cat} = k^{LE}/k^{HE}$) reported previously for fully labeled wild type EcDHFR[21,29] and in agreement with the implication of conformational changes in the N-terminal peptide during turnover. In contrast, the steady state rate constants for CT-EcDHFR (k_{cat}^{CT}) only deviate mildly from those of the 'light' enzyme, giving a maximum C-terminal kinetic isotope effect ($KIE_{cat}^{CT} = k_{cat}^{LE}/k_{cat}^{CT}$) of 1.04 ± 0.02 at 40 ºC. This is similar to the KIE_{cat} measured for DHFRs that lack significant conformational changes during catalysis.[22,30,41,54]

These results demonstrate that segmental heavy isotope labeling can be used to localize effects of protein isotopic substitutions on millisecond conformational motions. The observation that KIE_{cat}^{NT} is temperature-dependent and accounts for almost the entire KIE_{cat} of EcDHFR, while KIE_{cat}^{CT} is close to unity and shows only a small dependence on temperature indicates that residues 1-28 undergo substantial movement during the catalytic turnover. X-ray crystallographic studies of EcDHFR demonstrated previously that a substantial movement of the M20 loop (residues 9-24) is required for product release, whereas only a minor rearrangement is seen in the FG loop in the C-terminal segment and other regions of the enzyme (Figure 1).[45] Solution NMR measurements revealed that various regions of the enzyme in the EcDHFR:NADPH:H_4F complex show conformational motions on the same timescale as product release.[45] Although a contribution from other regions of the enzyme, too subtle to be detected by the methodology used here, may be possible, the results suggest that the motions of the M20 loop are dominant in limiting k_{cat}. These results therefore confirm the central importance of motions of the M20 loop to the physical steps of catalysis;[21] in addition, they are able to pinpoint the specific regions of the enzyme whose motions limit the observed rate constant for product release and hence k_{cat}, and distinguish them from other regions whose motions are on the same timescale as the observed rate constant but do not limit it.

To localize the origin of the fast motions that couple to the chemical step in the catalytic cycle, hydride transfer from NADPH to predominately protonated dihydrofolate, pre-steady-state stopped-flow kinetic measurements were performed at pH 7.0. The hydride transfer rate constants (k_H^{LE}) for unlabeled, ligated EcDHFR are in good agreement with those measured for the wild type enzyme (Figure S6 and Table S3).[55] The hydride transfer rate constants for NT-EcDHFR (k_H^{NT}) are identical to those measured for unlabeled, ligated EcDHFR giving a KIE_H^{NT} (k_H^{LE}/k_H^{NT}) close to unity at all temperatures (Figures 3 and S5). In contrast, measurable reactivity differences for CT-EcDHFR were observed with an isotope effect KIE_H^{CT} (k_H^{LE}/k_H^{CT}) that increases from 0.90 ± 0.02 at 5 ºC to 1.13 ± 0.08 at 35 ºC. Both the magnitude and temperature dependence of KIE_H^{CT} were similar to those of the enzyme KIE measured for fully labeled, wild type EcDHFR.[21] Indeed, the difference in the activation energies between the 'light', chemically ligated enzyme and CT-EcDHFR is statistically identical to that between the 'light' and 'heavy' wild type enzyme (Table 1). In contrast, this parameter is not affected by labeling the N-terminal segment of the chemically ligated enzyme. These observations provide strong evidence for dynamic coupling of the C-terminal region of EcDHFR to the chemical coordinate at pH 7.0; no evidence for such a coupling to the first 28 amino acid residues was found.

To confirm that the measured kinetic difference is an indication of dynamic effects, computational studies were performed. Enzyme hydride transfer rate constants can be estimated in the framework of Transition State Theory (TST), which includes a temperature-dependent transmission coefficient to account for tunneling contributions and dynamic effects:[18,56]

$$k_{H,theor}(T) = \Gamma(T,\xi)\frac{k_B T}{h} e^{-\left(\frac{\Delta G_{act}^{QC}(T,\xi)}{RT}\right)} \quad (1)$$

where R is the ideal gas constant, T is the temperature, k_B is the Boltzmann constant and h is Planck's constant. ΔG_{act}^{QC} is the quasiclassical activation free energy calculated along the reaction coordinate ξ:[18]

$$\Delta G_{act}^{QC}(T,\xi) = \Delta G_{act}^{CM}(T,\xi) + \Delta G_{vib}^{QM}(T) \quad (2)$$

where $\Delta G_{act}^{CM}(T,\xi)$ is the activation free energy obtained from classical simulations and $\Delta G_{vib}^{QM}(T)$ is a correction term due to the quantized nature of molecular vibrations (mainly zero-point energies). In eq. (1), $\Gamma(T,\xi)$ is the temperature-dependent transmission coefficient that contains dynamic and tunneling corrections to the classical rate constant and is therefore equal to one in the limit of classical TST. $\Gamma(T,\xi)$ can be expressed as:

$$\Gamma(T,\xi) = \gamma(T,\xi) \cdot \kappa(T) \quad (3)$$

where $\kappa(T)$ is the tunneling coefficient that accounts for reactive trajectories that do not reach the classical threshold energy. $\gamma(T,\xi)$ is the recrossing transmission coefficient that corrects the rate constant for the trajectories that recross the dividing surface from the product valley back to the reactant valley and that incorporates the participation of other coordinates during barrier crossing and frictional effects of the environment on the motion along ξ.

In principle, protein isotopic labeling can modify all the variables in eq. (2) and (3). Although isotopic labeling should not affect the activation free energy $\Delta G_{act}^{CM}(T,\xi)$ within the classical limit (if the mass associated with ξ is unaltered), quantum

vibrational averaged reduction of the C-H bond distance caused by deuterium substitution can theoretically change the magnitude of this variable. However, experimental[24,25] and theoretical studies[21] suggested that deuterium substitution should not alter electrostatic properties of the active site and consequently the activation free energy. Furthermore, QM/MM simulations of EcDHFR[21] and its catalytically compromised N23PP/S148A variant,[22] as well as DHFR from *Geobacillus stearothermophilus* (BsDHFR),[23] revealed that the tunneling coefficient is not altered by protein isotope labeling, thus excluding contributions from 'promoting vibrations' enhancing tunneling effects and related concepts.[36-41] Instead, the subtle difference in the rate constants of hydride transfer is mainly caused by a change in the recrossing trajectories and hence the enzymatic KIE_H can be approximated by the ratio of the recrossing transmission coefficients of the 'light' enzyme to that of the isotopically labeled, 'heavy' enzyme:[21-23]

$$KIE_H = \frac{k_H^{LE}}{k_H^{HE}} \approx \frac{\gamma^{LE}}{\gamma^{HE}} \quad (4)$$

Accordingly, the segment isotope effects were calculated by evaluating the recrossing transmission coefficients of 'light' EcDHFR, NT- and CT-EcDHFR from 278 to 318 K (Figure S7, Table 1 and S4). Computational segmental KIE_H values estimated from eq. (4) are presented in Figure 2 and follow the same trend as the experimental values obtained under pre-steady state conditions. Isotope labeling of the C-terminal fragment caused a greater difference in the recrossing coefficients and consequently a larger isotope effect at high temperature, while contributions from the N-terminal fragment are small. However, theoretical estimations always yield a normal enzyme KIE_H, where the hydride transfer reaction catalyzed by the 'light' enzyme is faster than that of the isotopically labeled enzyme. This can be explained by assuming ~~is based on the assumption that~~ the slower environment in the labeled enzyme increase~~s~~ing the friction of the reaction coordinate, resulting in a greater fraction of recrossing trajectories and a lower value of the rate constant. The experimental values on the other hand show an inverse effect at temperatures below 20 ºC. This could be an indication of additional contributions to the enzyme KIE_H, which cannot be explained by dynamic recrossing. In fact, heavy isotopic substitution could also modify the zero-point energies of the reactants and transition state differently, further changing the value of $\Delta G_{vib}^{QM}(T)$. A tighter interaction of the isotopically labeled enzyme with the transition state could result in an inverse KIE. However, previous analysis showed that, ~~so~~ as long as isotopic labeling does not involve the reacting fragments, this effect is small.[22] Consequently, in this work our isotope effect calculations remain within the approximation of eq. (4), although including the isotope effect on changing the zero-point energies of the reactants and transition states in eq. (2) might yield more accurate predictions, especially the enzyme KIE_H at low temperature (because of the 1/T dependence in the exponential term).

The measured recrossing coefficients could also be used to explain the differences in the activation parameters. Both CT-EcDHFR and completely labeled 'heavy' EcDHFR have more negative activation entropies ($\Delta S^{\ddagger}$) than the 'light' enzymes (Table 1). $\Delta S^{\ddagger}$ is expected to be negative, because during the chemical transformation the enzyme needs to sacrifice its flexibility to provide a static, charge-complementary configuration.[23] However, the activation entropy is also affected by the intensity of dynamic coupling, as it is dependent on the magnitude and the temperature dependence of the recrossing coefficient, the contribution from which is described in equation (5):[23,57]

$$\Delta S^{\ddagger}(\gamma) = R \cdot \ln(\gamma) + \frac{RT}{\gamma} \cdot \frac{\partial \gamma}{\partial T} \quad (5)$$

where $\Delta S^{\ddagger}(\gamma)$ is the fraction of activation entropy that depends on dynamic recrossing and $\frac{\partial \gamma}{\partial T}$ is the change of the recrossing coefficient with temperature.

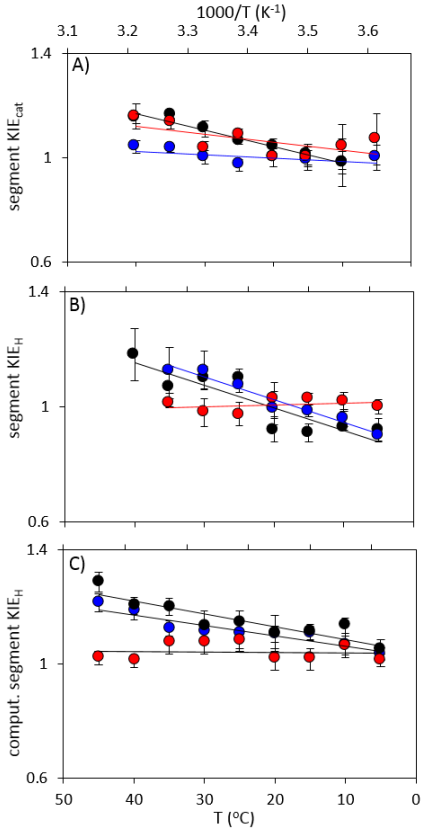

Figure 2. Enzyme and segment kinetic isotope effects measured at pH 7.0 for fully labeled EcDHFR (black),[21] NT-EcDHFR (red) and CT-EcDHFR (blue) under steady state (A) and single turnover, pre-steady state (B) conditions. Theoretical isotope effects (C) calculated from the ratios of the recrossing coefficients (eq. 4).

As illustrated in the computational analysis, the recrossing coefficient deviates further from unity with increasing temperature (*i.e.* $\frac{\partial \gamma}{\partial T} < 0$) due to thermal activation of protein motions that disturb the stability of the transition state. This effect is particularly pronounced in 'heavy' EcDHFR and in CT-EcDHFR, and the magnitude of $\frac{\partial \gamma}{\partial T}$ is approximately three-fold higher than for the 'light' enzyme (Table S4). Consequently, the activation entropies of these isotopically labeled enzymes are greater in magnitude and the hydride transfer rate constant becomes more noticeably lower than for the 'light' enzyme at high temperature. Nevertheless, the activation free energies ($\Delta G^{\ddagger}$) are identical for these enzymes as the activation enthalpies ($\Delta H^{\ddagger}$) of both 'heavy' EcDHFR and CT-EcDHFR are lower than their 'light' counterparts. On the other hand, the

activation free energy also remains unchanged in NT-EcDHFR since none of the mentioned parameters were affected by isotope labeling. These observations strongly suggest that the protein environmental motions along the EcDHFR reaction coordinate originate from the C-terminal segment.

Table 1. Kinetic parameters for the hydride transfer reactions catalyzed by various forms of EcDHFR at 25 ºC.

Enzymes	E_A (kcal·mol^{-1})	ΔE_A (kcal·mol^{-1})	$\Delta S^{\ddagger}$ (cal·mol^{-1}·K^{-1})	$\Delta\Delta S^{\ddagger}$ (cal·mol^{-1}·K^{-1})	$\Delta H^{\ddagger}$ (kcal·mol^{-1})	$\Delta\Delta H^{\ddagger}$ (kcal·mol^{-1})	$\Delta G^{\ddagger}$ (kcal·mol^{-1})
Light WT EcDHFR[a]	7.3 ± 0.2		-26 ± 1		6.7 ± 0.3		14.4 ± 1.5
Heavy WT EcDHFR[a]	6.0 ± 0.3	1.3 ± 0.4	-30 ± 2	4 ± 2	5.4 ± 0.6	1.3 ± 0.7	14.4 ± 2.5
Light, chemically ligated EcDHFR-A29C	8.3 ± 0.3		-22 ± 1		7.8 ± 0.3		14.3 ± 1.3
NT-EcDHFR	8.4 ± 0.2	0.1 ± 0.4	-22 ± 2	0 ± 2	7.8 ± 0.6	0 ± 0.7	14.3 ± 1.9
CT-EcDHFR	7.0 ± 0.4	1.3 ± 0.5	-27 ± 2	5 ± 2	6.5 ± 0.8	1.3 ± 0.9	14.3 ± 3.5
a) Data from ref (21)							

Measurement of segmental KIE_H provides new information about the nature of dynamic coupling to the chemical step of EcDHFR catalysis. Several residues implicated in the proposed 'hydride transfer driving' dynamic network are located in the M20 loop (residues 9-23)[36-41] and a measureable KIE_H^{NT} would be expected if dynamic coupling from these residues to the chemical step were present. For instance, Tyr100 and the hydrogen-bonding network between Ile14, Gly15 and Asp122 were proposed to 'direct' NADPH to the acceptor,[37] while Phe31 and the interactions between Trp22, Asp27 and Thr113 'direct' H_2F to the donor. Dynamic coupling to the actual chemical step at pH 7.0 however does not involve the first 28 amino acids of EcDHFR, despite this N-terminal region showing the largest thermal motions; it originates exclusively from within the C-terminal region. These movements involving the M20 loop therefore generate a reaction-ready active site configuration, from which hydride transfer can take place,[17,22,29,46] but they do not significantly couple to the reaction coordinate. This work provides the first direct experimental evidence, which regions of EcDHFR couple to the hydride transfer event itself. Furthermore, based on these results we hypothesize that the observed dynamic effects originate from a reorganisation that facilitates the charge transfers necessary to form the transition state configuration and/or tight protein interactions with the transition state. Furthermore, we hypothesize that the observed dynamic effects are 'residual' motions caused by tight electrostatic interactions between the enzyme and transition state species. Dynamic coupling is an undesired effect that enhances dynamic recrossing and most likely causes an additive effect to the magnitude of enzyme KIE_H.

Site-directed mutagenesis has often been used to investigate the role and existence of dynamic effects in enzyme catalysis.[35,41,58] However, mutations can alter an enzyme's electrostatic properties and barriers for conformational and chemical transitions,[43,59,60] making these studies potentially controversial since differentiating electrostatic and dynamic effects is often difficult. In contrast, protein isotopic labeling shows negligible changes to the electrostatic properties but slows protein motions on all timescales. Hence, segment isotope effects are a practical method to investigate dynamic effects on enzyme catalysis with spatial resolution. They can identify regions of an enzyme that couple to the reaction coordinate and can distinguish regions of the enzyme involved in millisecond conformational motions from those whose fast dynamics couple to barrier crossing. The results presented here reveal that at physiological pH the release of H_4F from the ternary EcDHFR:NADPH:H_4F product complex is dominated by millisecond conformational motions of the M20 loop with minimal contribution from other regions of the enzyme. In stark contrast, motions of C-terminal portions of the enzyme affect the chemical step while motions of the M20 loop do not make significant measurable contributions to hydride transfer itself.

Segmental heavy isotope labeling is capable of isolating individual contributions of different regions of an enzyme to the observed rate constants and, when complemented with computational studies,[11-13,19,20,32,36,42,44] provides insights not easily obtained with other methods. The concept of segmental heavy isotope labeling may help the design and development of inhibitors of motions crucial for the catalytic cycle. Most importantly, the current study demonstrates the applicability of segment isotope labeling to studies of a wide variety of models in the field of protein dynamics and beyond.

ASSOCIATED CONTENT

Supporting Information

Full experimental procedures, mass spectra of purified proteins, circular dichroism spectra, tabulated experimental data for k_H, k_{cat}, and enzyme KIEs, pH dependence of k_H, computational methodology and theoretical estimations of the transmission coefficients for the light, heavy, CT and NT labeled versions of the enzyme. This material is available free of charge via the Internet at http://pubs.acs.org.

AUTHOR INFORMATION

Corresponding Authors

allemannrk@cardiff.ac.uk
moliner@uji.es
ignacio.tunon@uv.es

Notes

Any additional relevant notes should be placed here.

ACKNOWLEDGMENT

This work was supported by Cardiff University, grants BB/J005266/1 and BB/L020394/1 (R.K.A.) from the UK's Biotechnology and Biological Sciences Research Council (BBSRC), by FEDER and Ministerio de Economía y Competitividad funds (project CTQ2012-36253-C03), Generalitat Valenciana

(ACOMP/2014/277 and PrometeoII/2014/022) and by Universitat Jaume I (Project P1·1B2011-23). The authors acknowledge computational resources from the University of Valencia (Tirant supercomputer).

REFERENCES

(1) Koshland, D. E. *Proc. Natl. Acad. Sci. USA* **1958**, *44*, 98.
(2) Henzler-Wildman, K.; Lei, M.; Thai, V.; Kerns, S. J.; Karplus, M.; Kern, D. *Nature* **2007**, *450*, 913.
(3) Boehr, D. D.; McElheny, D.; Dyson, H. J.; Wright, P. E. *Science* **2006**, *313*, 1638.
(4) Henzler-Wildman, K. A.; Thai, V.; Lei, M.; Ott, M.; Wolf-Watz, M.; Fenn, T.; Pozharski, E.; Wilson, M. A.; Petsko, G. A.; Karplus, M.; Hubner, C. G.; Kern, D. *Nature* **2007**, *450*, 838.
(5) Peng, J. W. *Structure* **2009**, *17*, 319.
(6) Basran, J.; Sutcliffe, M. J.; Scrutton, N. S. *Biochemistry* **1999**, *39*, 3218.
(7) Antoniou, D.; Caratzoulas, S.; Kalyanaraman, C.; Mincer, J. S.; Schwartz, S. D. *Eur. J. Biochem.* **2002**, *269*, 3103.
(8) Sutcliffe, M. J.; Scrutton, N. S. *Eur. J. Biochem.* **2002**, *269*, 3096.
(9) Knapp, M. J.; Klinman, J. P. *Eur. J. Biochem.* **2002**, *269*, 3113.
(10) Klinman, J. P. *J. Phys. Org. Chem.* **2010**, *23*, 606.
(11) Adamczyk, A. J.; Cao, J.; Kamerlin, S. C. L.; Warshel, A. *Proc. Natl. Acad. Sci. USA* **2011**, *108*, 14115.
(12) Pisliakov, A. V.; Cao, J.; Kamerlin, S. C. L.; Warshel, A. *Proc. Natl. Acad. Sci. USA* **2009**, *106*, 17359.
(13) Boekelheide, N.; Salomón-Ferrer, R.; Miller, T. F. *Proc. Natl. Acad. Sci. USA* **2011**, *108*, 16159.
(14) Loveridge, E. J.; Allemann, R. K. *Biochemistry* **2010**, *49*, 5390.
(15) Loveridge, E. J.; Tey, L.-H.; Allemann, R. K. *J. Am. Chem. Soc.* **2010**, *132*, 1137.
(16) Loveridge, E. J.; Tey, L.-H.; Behiry, E. M.; Dawson, W. M.; Evans, R. M.; Whittaker, S. B.-M.; Gunther, U. L.; Williams, C.; Crump, M. P.; Allemann, R. K. *J. Am. Chem. Soc.* **2011**, *133*, 20561.
(17) Loveridge, E. J.; Behiry, E. M.; Guo, J.; Allemann, R. K. *Nat. Chem.* **2012**, *4*, 292.
(18) Alhambra, C.; Corchado, J.; Sanchez, M. L.; Garcia-Viloca, M.; Gao, J.; Truhlar, D. G. *J. Phys. Chem. B* **2001**, *105*, 11326.
(19) Pu, J.; Ma, S.; Gao, J.; Truhlar, D. G. *J. Phys. Chem. B* **2005**, *109*, 8551.
(20) Cui, Q.; Karplus, M. *J. Phys. Chem. B* **2002**, *106*, 7927.
(21) Luk, L. Y. P.; Ruiz-Pernia, J. J.; Dawson, W. M.; Roca, M.; Loveridge, E. J.; Glowacki, D. R.; Harvey, J. N.; Mulholland, A. J.; Tuñón, I.; Moliner, V.; Allemann, R. K. *Proc. Natl. Acad. Sci. USA* **2013**, *110*, 16344.
(22) Ruiz-Pernia, J. J.; Luk, L. Y. P.; García-Meseguer, R.; Martí, S.; Loveridge, E. J.; Tuñón, I.; Moliner, V.; Allemann, R. K. *J. Am. Chem. Soc.* **2013**, *135*, 18689.
(23) Luk, L. Y. P.; Ruiz-Pernía, J. J.; Dawson, W. M.; Loveridge, E. J.; Tuñón, I.; Moliner, V.; Allemann, R. K. *J. Am. Chem. Soc.* **2014**, *136*, 17317.
(24) Silva, R. G.; Murkin, A. S.; Schramm, V. L. *Proc. Natl. Acad. Sci. USA* **2011**, *108*, 18661.
(25) Kipp, D. R.; Silva, R. G.; Schramm, V. L. *J. Am. Chem. Soc.* **2011**, *133*, 19358.
(26) Pudney, C. R.; Guerriero, A.; Baxter, N. J.; Johannissen, L. O.; Waltho, J. P.; Hay, S.; Scrutton, N. S. *J. Am. Chem. Soc.* **2013**, *135*, 2512.
(27) Toney, M. D.; Castro, J. N.; Addington, T. A. *J. Am. Chem. Soc.* **2013**, *135*, 2509.
(28) Świderek, K.; Javier Ruiz-Pernía, J.; Moliner, V.; Tuñón, I. *Curr. Op. Chem. Biol.* **2014**, *21*, 11.
(29) Wang, Z.; Singh, P. N.; Czekster, C. M.; Kohen, A.; Schramm, V. L. *J. Am. Chem. Soc.* **2014**, *136* 8333.
(30) Luk, L. Y. P.; Loveridge, E. J.; Allemann, R. K. *J. Am. Chem. Soc.* **2014**, *136*, 6862.
(31) Garcia-Viloca, M.; Truhlar, D. G.; Gao, J. *Biochemistry* **2003**, *42*, 13558.
(32) Liu, H.; Warshel, A. *J. Phys. Chem. B* **2007**, *111*, 7852.
(33) Cameron, C. E.; Benkovic, S. J. *Biochemistry* **1997**, *36*, 15792.
(34) Wang, L.; Tharp, S.; Selzer, T.; Benkovic, S. J.; Kohen, A. *Biochemistry* **2006**, *45*, 1383.
(35) Singh, P.; Sen, A.; Francis, K.; Kohen, A. *J. Am. Chem. Soc.* **2014**, *136*, 2575.
(36) Watney, L. B.; Agarwal, P. K.; Hammes-Schiffer, S. *J. Am. Chem. Soc.* **2003**, *125*, 3745.
(37) Agarwal, P. K.; Billeter, S. R.; Rajagopalan, P. T. R.; Benkovic, S. J.; Hammes-Schiffer, S. *Proc. Natl. Acad. Sci. USA* **2002**, *99*, 2794.
(38) Radkiewicz, J. L.; Brooks III, C. L. *J. Am. Chem. Soc.* **2000**, *122*, 225.
(39) Rod, T. H.; Radkiewicz, J. L.; Brooks III, C. L. *Proc. Natl. Acad. Sci. USA* **2003**, *100*, 6980.
(40) Stojković, V.; Perissinotti, L. L.; Lee, J.; Benkovic, S. J.; Kohen, A. *Chem. Commun* **2010**, *46*, 8974.
(41) Bhabha, G.; Lee, J.; Ekiert, D. C.; Gam, J.; Wilson, I. A.; Dyson, H. J.; Benkovic, S. J.; Wright, P. E. *Science* **2011**, *332*, 234.
(42) Fan, Y.; Cembran, A.; Ma, S.; Gao, J. *Biochemistry* **2013**, *52*, 2036.
(43) Roston, D.; Kohen, A.; Doron, D.; Major, D. T. *J Computat. Chem.* **2014**, *35*, 1411.
(44) Arora, K.; Brooks Iii, C. L. *J. Am. Chem. Soc.* **2009**, *131*, 5642.
(45) Fierke, C. A.; Johnson, K. A.; Benkovic, S. J. *Biochemistry* **1987**, *26*, 4085.
(46) Sawaya, M. R.; Kraut, J. *Biochemistry* **1997**, *36*, 586.
(47) Bhabha, G.; Ekiert, D. C.; Jennewein, M.; Zmasek, C. M.; Tuttle, L. M.; Kroon, G.; Dyson, H. J.; Godzik, A.; Wilson, I. A.; Wright, P. E. *Nat Struct Mol Biol* **2013**, *20*, 1243.
(48) Behiry, E. M.; Luk, L. Y. P.; Matthews, S. M.; Loveridge, E. J.; Allemann, R. K. *Biochemistry* **2014**, *53*, 4761.
(49) Epstein, D. M.; Benkovic, S. J.; Wright, P. E. *Biochemistry* **1995**, *34*, 11037.
(50) Dawson, P.; Muir, T.; Clark-Lewis, I.; Kent, S. *Science* **1994**, *266*, 776.
(51) Torbeev, V. Y.; Raghuraman, H.; Hamelberg, D.; Tonelli, M.; Westler, W. M.; Perozo, E.; Kent, S. B. H. *Proc. Natl. Acad. Sci. USA* **2011**, *108*, 20982.
(52) Valiyaveetil, F. I.; Sekedat, M.; MacKinnon, R.; Muir, T. W. *J. Am. Chem. Soc.* **2006**, *128*, 11591.
(53) Ottesen, J. J.; Bar-Dagan, M.; Giovani, B.; Muir, T. W. *Pept. Science* **2008**, *90*, 406.
(54) Dams, T.; Bohm, G.; Auerbach, G.; Bader, G.; Schurig, H.; Jaenicke, R. *Biol. Chem.* **1998**, *379*, 367.
(55) Swanwick, R. S.; Maglia, G.; Tey, L.; Allemann, R. K. *Biochem. J.* **2006**, *394*, 259.
(56) Truhlar, D. G.; Garrett, B. C.; Klippenstein, S. J. *J. Phys. Chem.* **1996**, *100*, 12771.
(57) Pu, J.; Gao, J.; Truhlar, D. G. *Chem. Rev.* **2006**, *106*, 3140.
(58) Wang, L.; Goodey, N. M.; Benkovic, S. J.; Kohen, A. *Proc. Nat. Acad. Sci. U.S.A.* **2006**, *103*, 15753.
(59) Swanwick, R. S.; Shrimpton, P. J.; Allemann, R. K. *Biochemistry* **2004**, *43*, 4119.
(60) Boehr, D. D.; Schnell, J. R.; McElheny, D.; Bae, S.-H.; Duggan, B. M.; Benkovic, S. J.; Dyson, H. J.; Wright, P. E. *Biochemistry* **2013**, *52*, 4605.

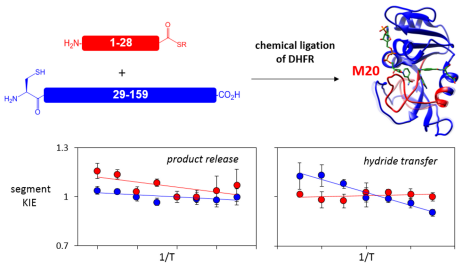
1-28
29-159
chemical ligation
of DHFR
M20
product release
hydride transfer
segment
KIE
1.3
1
0.7
1/T
1/T